Visualizing curved spacetime

Rickard M. Jonsson

Department of Astronomy and Astrophysics, Physics and Engineering Physics, Chalmers University of Technology, and Göteborg University, 412 96 Gothenburg, Sweden

E-mail: rico@fy.chalmers.se

Abstract. I present a way to *visualize* the concept of curved spacetime. The result is a curved surface with local coordinate systems (Minkowski Systems) living on it, giving the local directions of space and time. Relative to these systems, special relativity holds. The method can be used to visualize gravitational time dilation, the horizon of black holes, and cosmological models. The idea underlying the illustrations is first to specify a field of timelike four-velocities u^μ. Then, at every point, one performs a coordinate transformation to a local Minkowski system comoving with the given four-velocity. In the local system, the sign of the spatial part of the metric is flipped to create a new metric of Euclidean signature. The new positive definite metric, called the *absolute* metric, can be covariantly related to the original Lorentzian metric. For the special case of a 2-dimensional original metric, the absolute metric may be embedded in 3-dimensional Euclidean space as a curved surface.

I   Introduction

Einstein's theory of gravity is a geometrical theory and is well suited to be explained by images. For instance the way a star affects the *space* around it can easily be displayed by a curved surface. The very heart of the theory, the *curved spacetime*, is however fundamentally difficult to display using curved surfaces. The reason is that the Lorentz signature gives us negative squared distances, something that we never have on ordinary curved surfaces.

However, we can illustrate much of the spacetime structure using flat diagrams that include the lightcones. Famous examples of this are the Kruskal and Penrose diagrams (see e.g. Ref. 1). Such pictures are valuable tools for understanding black holes.

In this article I will describe a method that lets us visualize not just the causal structure of spacetime, but also the scale (the proper distances). It is my hope that these illustrations can be of help in explaining the basic concepts of general relativity to a general audience.

In exploring the possibilities of this method I use the language and mathematics of general relativity. The level is that of teachers (or skilled students) of general relativity.

The resulting illustrations can however be used without any reference to mathematics to explain concepts like gravitational time dilation, cosmological expansion, horizons and so on.

In Sec. II, I give a brief introduction to the concept of curved spacetime, using the method of this article, and consider a few examples of physical interest. This section presumes no knowledge of general relativity. In Sec. III, I explain the method underlying the illustrations thus far, and also apply it to a black hole and a hollow star. In Secs. IV-VIII, I present the general formalism, demonstrate how to use it to produce embeddings and investigate the geodesic properties of the formalism. These sections are of a more technical character. In Secs. IX-XIII, I apply the formalism to various types of spacetimes. In Secs. XIV-XVI, I relate this work to other similar approaches, and comment on this article. Secs. XVII and XVIII include some pedagogical questions and answers.

II   Introduction to curved spacetime

Consider a clock moving along a straight line. Special relativity tells us that the clock will tick more slowly than the clocks at rest as illustrated in Fig. 1.
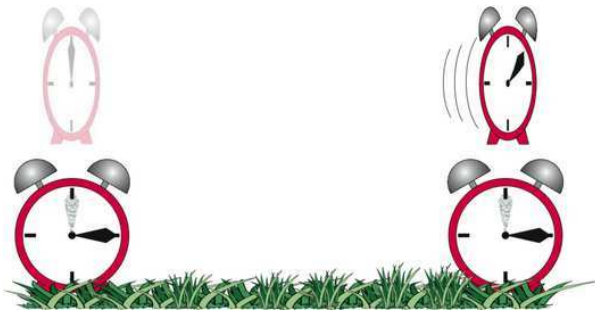

Figure 1: A clock moving along a straight line. Relative to the clocks at rest, the moving clock will tick more slowly.

Consider two events on the moving clock, separated by a time dt and a distance dx, as seen relative to the system at rest. We can illustrate the two events, and the motion of the clock in a *spacetime diagram* as depicted in Fig. 2. Time is directed upwards in the diagram. The motion of the clock corresponds to a *worldline* in the diagram.

The proper time interval $d\tau$ is the time between the two events according to the moving clock, which is given by[2]

$$d\tau^2 = dt^2 - \left(\frac{dx}{c}\right)^2. \tag{1}$$

Here c is the velocity of light. Note that in the limit as the speed of the clock approaches the speed of light we have $dx = cdt$, and thus from Eq. (1) we have $d\tau = 0$. A clock moving almost at the speed of light will thus almost not tick at all relative to the clocks at rest.
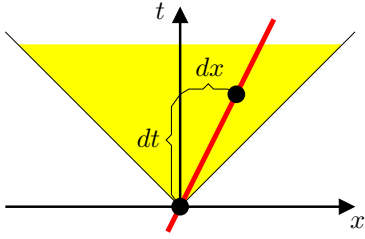
Figure 2: A spacetime diagram showing the worldline of the moving clock (the fat line). The two events we are considering are the black dots in the diagram. The shaded area is known as the lightcone.

It is customary to choose the axes of the spacetime diagram in such a manner that motion at the speed of light corresponds to a line that is inclined at a 45° angle relative to the axes of the diagram. At every point in the diagram we can then draw a little triangle, with a 90° opening angle, known as a lightcone. The rightmost edge of the triangle corresponds to a right-moving photon and the leftmost edge corresponds to a left-moving photon. No material objects can travel faster than the velocity of light, which means that the worldlines of objects must always be directed within the local lightcone.

A   Curved spacetime

In general relativity we have a *curved* spacetime, which we may illustrate by a curved surface with little locally flat coordinate systems, known as Minkowski systems, living on it as illustrated in Fig. 3.
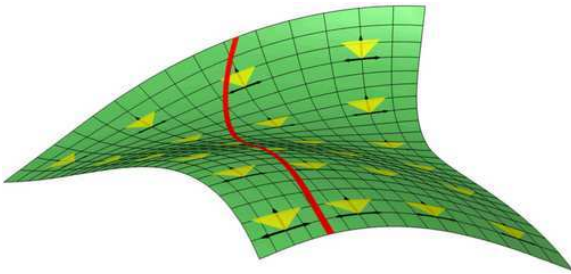

Figure 3: An illustration of curved spacetime using a curved surface with little Minkowski systems living on it. The curving line could be the worldline of a moving clock.

The little coordinate systems on the surface work precisely as the spacetime diagram of Fig. 2. In particular the worldlines of moving objects must always be directed within the local lightcone. To find out how much a clock has ticked along it's winding worldline, we consider nearby events along the worldline and sum up the $d\tau$'s we get using Eq. (1), where dt and dx are the time and space separation between the events as seen relative to the local Minkowski system.

B   The spacetime of a line through a dense star

As a specific example let us consider the spacetime of a line through a very dense star as depicted in Fig. 4.
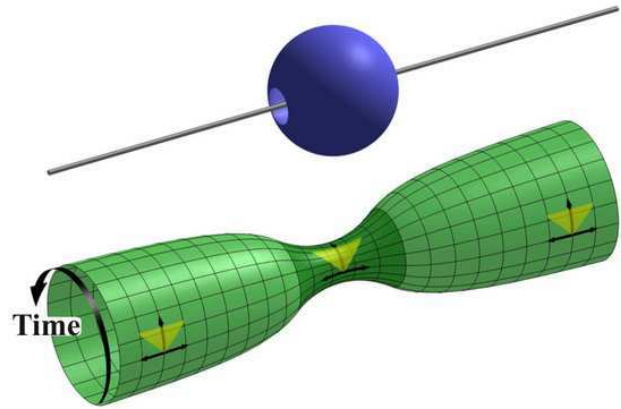

Figure 4: A radial line through a very dense star, and an illustration of the curved spacetime for that line. Time is directed around the hourglass shaped surface. Strictly speaking the surface should not close in on itself in the time direction. Rather one should come to a new layer after one circumference as on a paper roll.

The circles around the surface correspond to fixed positions along the line through the star. The lines directed along (as opposed to around) the surface correspond to fix coordinate time (known for this particular case as Schwarzschild time).

Consider now two observers, one at rest in the middle of the star and the other at rest far to the left of the star. The worldlines of these observers are circles around the middle and the left end of the spacetime. Obviously the distance measured around the spacetime is shorter at the middle than at the end. This means that the proper time (the experienced time) per turn around the spacetime is shorter in the middle than at the end. From this we may understand that time inside the star runs slow relative to time outside the star.

To be more specific consider the following scenario. Let an observer far outside the star send two photons, separated by a time corresponding to one lap, towards the center of the star. The corresponding worldlines of the photons will spiral around the surface and arrive at the center of the star still separated by one lap. The points where the photons arrive at the center will in this illustration be the same, but they are different points in spacetime because the surface is layered as in a paper roll. Since the distance around the central part of the spacetime is smaller than that towards the ends of the spacetime the observer in the center of the star will experience a shorter time between the arrival of the two photons than the time between the emission of the two photons, as experienced by the sender. This effect is known as gravitational time

dilation – and is a consequence of the shape of spacetime.

Alternatively we may note that the lines of constant coordinate time are lying closer to each other in the middle of the spacetime surface than at the ends. An observer inside the star will therefore observe that a local clock showing Schwarzschild coordinate time (synchronized with a proper clock far outside the star) ticks much faster than a clock measuring proper time within the star. We may then understand that an observer inside the star will see the Universe outside the star evolving at a faster rate than that experienced by an observer outside the star.

C   Freely falling motion

According to general relativity, an object thrown out radially from the surface of the star, moving freely (so there is no air resistance for instance), takes a path through spacetime such that the proper time elapsed along the worldline of the object is *maximized*. Consider then two events, at the surface of the star separated by some finite time only. It is easy to imagine that a particle traveling between the two events will gain proper time by moving out towards a larger embedding radius (where the circumference is greater), before moving back to the second event. On the other hand it cannot move out too fast since then it will move at a speed too close to the speed of light – whereby the internal clock hardly ticks at all, see Fig. 5.
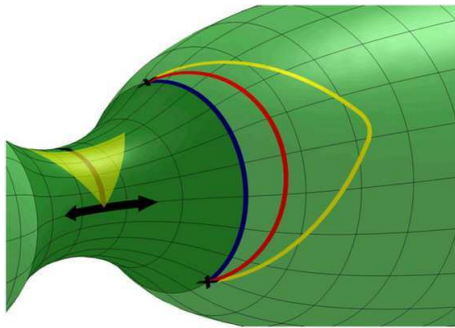

Figure 5: Three different worldlines connecting two fixed events. The middle worldline corresponds to the actual motion of an object initially thrown radially away from the star and then falling back towards the star. Of the three worldlines this has the largest integrated proper time.

To predict the motion of an object that has been thrown out from the star and returns to the same location after a specific amount of time, we can in principle consider different pairs of events (as in Fig. 5), find the worldline that maximizes the integrated proper time. This trajectory corresponds to the motion that we are seeking. Thus we can explain not only gravitational time dilation but also the motion of thrown objects using images of the type shown in Fig. 4 and Fig. 5.

D   Cosmological models

We may use the the same technique that we employed in the previous section to visualize the spacetimes corresponding to various cosmological models (although we are restricted to one spatial dimension). In Fig. 6, a few images of such models are displayed.
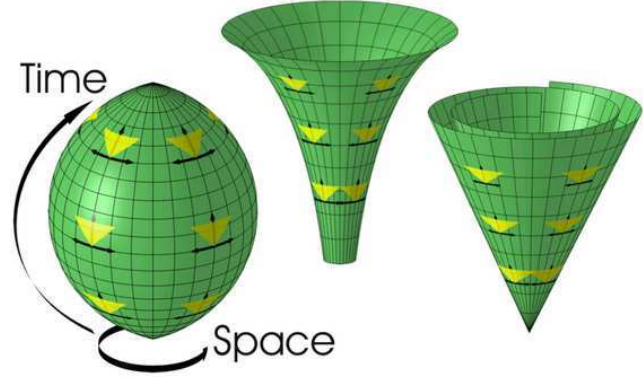

Figure 6: Schematic spacetime cosmological models.

Notice that time is here directed along the surface and space is directed around the surface. Just like before the local coordinate systems, in which special relativity holds, gives the local spatial and temporal distances.

The leftmost illustration corresponds to a Big Bang and Big Crunch spacetime. As we follow the spacetime upwards (i.e forward in time) the circumference first increases and then shrinks. This means that space itself expands and then contracts. The Big Bang is here just a point on the spacetime – where the spatial size of the universe was zero. I will leave it to the reader to describe how space behaves in the two rightmost spacetimes.

Using Newtonian intuition one might think of the Big Bang as a giant fire cracker exploding at some point in time. As the fire cracker explodes it sends out a cloud of particles that expands at a great rate relative to a *fixed* space. In Einstein's theory it is space itself that expands due to the *shape* of spacetime. Also unlike in the fire cracker view we cannot in general even talk about a time before the Big Bang in Einstein's theory.

As another application of the illustrations of Fig. 6, consider a set of photon worldlines separated by some small spatial distance shortly after the Big Bang in the leftmost Big Bang model. The worldlines will spiral around the spacetime, always at 45° to the local time axis. From this we may understand that they will get further and further separated as the circumference of the universe increases. Thinking of a photon as a set of wave crests that are all moving at the speed of light, we then understand that the wavelength of a photon will get longer and longer as the universe grows larger. This effect is known as the cosmological red shift. We can consider a similar scenario for the gravitational redshift by considering a photon moving along the spacetime of the line through the dense star of Fig. 4.

III   A simple method

The idea allowing us to make a figure like Fig. 4, which is an exact representation of the spacetime geometry, is simple. Assume that we have a two-dimensional, Lorentzian, time-independent and diagonal metric:

$$d\tau^2 = g_{tt}dt^2 + g_{xx}dx^2. \tag{2}$$

We then produce a new metric by taking the absolute value of the original metric components:

$$d\bar{\tau}^2 = |g_{tt}|dt^2 + |g_{xx}|dx^2. \tag{3}$$

The new metric, called the absolute metric, is positive definite and can be embedded in three dimensional Euclidean space as a surface of revolution because g_{tt} and g_{xx} are independent of t. For an observer with fixed x, pure temporal and pure spatial distances will precisely correspond to the absolute distances. There will thus be small Minkowski systems living on the curved surface. Analogous arguments hold if we have x rather than t-independence (as for the cosmological models).

A   Black hole embedding

As another example of the visualization scheme outlined above, we consider the line element of a radial line through a Schwarzschild black hole. An embedding of the corresponding absolute metric is depicted in Fig. 7.
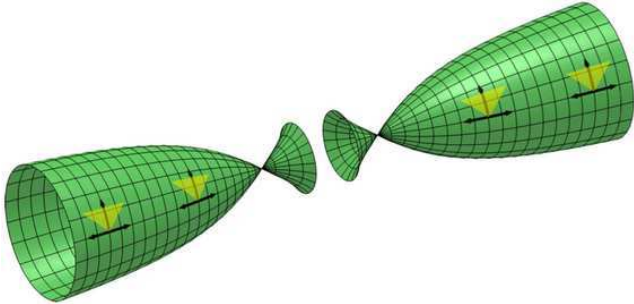

Figure 7: An embedding of the absolute spacetime of a central line through a black hole.

As before, the azimuthal angle corresponds to the Schwarzschild time. The two points of zero embedding radius correspond to the horizon on either side of the black hole. As we approach these points from the outside, the time dilation becomes infinite. The trumpet-like regions within these points lie within the horizon. Here moving *along* the surface (as opposed to moving around the surface) corresponds to timelike motion.

Photons, however, move at a 45° angle relative to a purely azimuthal line, both inside and outside of the horizon. Studying a photon trajectory coming from the outside and spiraling towards the point of zero embedding radius, it is not hard to realize that it will take an infinite number of laps (i.e. infinite Schwarzschild time) to reach that point.

The singularity (where the spacetime curvature becomes infinite) is not visible in the picture. While the distance as measured along the internal trumpet from the horizon to the singularity is finite (it has to be since we know that the proper time to reach the singularity once inside the horizon is finite) the embedding radius is infinite at the singularity. Thus, we cannot show the singularity using this visualization. We can however come arbitrarily close by everywhere making the embedding radius smaller. In Fig. 8 we zoom in on the internal geometry.
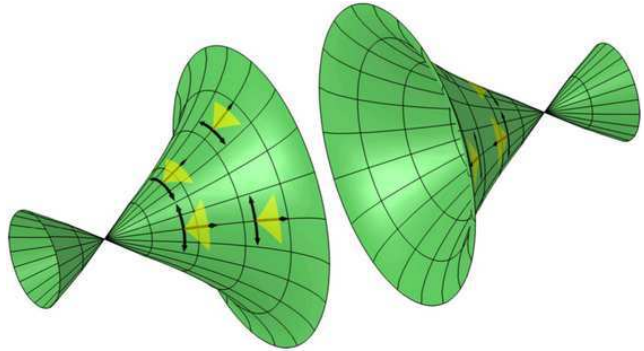

Figure 8: The absolute internal spacetime of a central line through a black hole. Notice the direction of the lightcones. The singularity lies in the (temporal) direction that the lightcones are opening up towards.

Note that the singularity is not a spatial point to which we may walk. Once inside the horizon, the singularity lies in the *future* and it is impossible to avoid it – just like it is impossible to avoid New Years Eve. In this 1+1 dimensional scenario (inside the horizon) the singularity is the time when space expands at an infinite rate.

Following a Schwarzschild time line (of fixed azimuthal angle) inside the black hole corresponds to timelike geodesic motion. Imagine then two trajectories directed along two such coordinate lines, starting close to the horizon and extending towards the singularity. The corresponding two observers will be at rest with respect to each other at the start (to zeroth order in the initial separation between them). As they approach the singularity they will however drift further and further apart in spacetime. At the singularity, where the embedding radius is infinite, they will be infinitely separated. We also know that the time it takes to reach the singularity is finite. It is then easy to imagine that if we try to keep the observers together, the force required will go to infinity as we approach the singularity. Hence, whatever we throw into a black hole will be ripped apart as it approaches the singularity. Notice however that there is no gravitational force in general relativity. The shape of spacetime is in this case simply such that a force is needed to keep things together, and in the end no force is strong enough.

B   Thin spherical crust

As a pedagogical example, imagine a hollow massive star, with a radial line through it, as illustrated in Fig. 9.
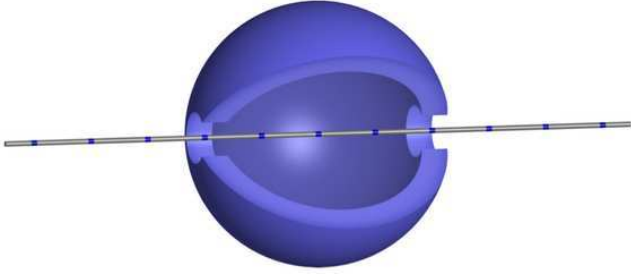

Figure 9: A line through a thin crust of high mass. The wedge is cut out to obtain a better view of the interior of the star.

We know from Birkhoff's theorem (see e.g. Ref. 3) that, assuming spherical symmetry, the spacetime outside the crust will match the external Schwarzschild solution. On the inside however, spacetime must be Minkowski.[4] In Fig. 10 the absolute spacetime of the radial line is displayed.
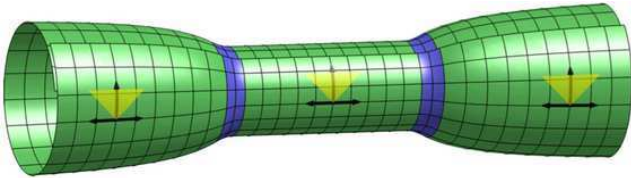

Figure 10: A schematic picture of the spacetime for a line through a hollow star in the absolute scheme. Notice how, after one circumference in time, we are really at a new layer.

If we were to cut out a square of the interior spacetime it would look just like a corresponding square cut out at infinity. There is thus no way that one, even by finite sized experiments (not just local experiments) within the crust, can distinguish between being inside the star or being at infinity. Even tidal effects are completely absent.

If we however were to open up a dialogue with someone on the outside, we would find that the outside person would talk very fast, and in a high pitched tone, whereas our speech would appear very slow and thick to the outside person.

The point that one can illustrate is that we do not have to feel gravity for it to be there. Gravity is not about forces pulling things, it is about the fabric of space and time, and how the different pieces of this fabric are woven together.

IV   Generalization to arbitrary spacetimes

The scheme outlined in the preceding section was specific for a particular type of metric expressed in a particular type of coordinates. There is however a way to generalize this scheme.

Given a Lorentzian spacetime of arbitrary dimensionality (although we commonly will apply the scheme to two dimensions), the idea is first to specify a field of timelike four-velocities denoted $u^\mu(x)$ (we will refer to spacetime velocities as four-velocities regardless of dimensionality). We then make a coordinate transformation to a local Minkowski system comoving with the given four-velocity at every point. In the local system we flip the sign of the spatial part of the metric to create a new *absolute* metric of Euclidean signature. Notice that the new metric will be highly dependent on our choice of generating four-velocities. The absolute metric together with the field of four-velocities contains all the information about the original spacetime, and allows one to keep track of what is timelike and what is not. We can always do the backwards transformation and flip the local positive definite metric into a Lorentzian (Minkowski) metric.

Considering for example the black hole illustrations of the preceding section, the *generators* (the worldlines tangent to the field u^μ) outside the horizon were simply those of the Schwarzschild observers at rest. Inside the horizon the generators were the worldlines of observers for whom $t = $ const. Notice that the observers located right outside the horizon have infinite proper acceleration. It is then perhaps not surprising that the resulting embedding is singular at the horizon. As we will see in Sec. V we can better resolve the horizon by using the worldlines of freely falling observers as generators.

A   A covariant approach

We could carry out the scheme we just outlined explicitly, doing coordinate transformations, flipping the sign of the metric and transforming it back again. There is, however, a more elegant method. We know that the absolute metric, from now on denoted by $\bar{g}_{\mu\nu}$, is a tensor (as any metric), and in a frame comoving with u^μ we have

$$\bar{g}_{\mu\nu} = \begin{bmatrix} 1 & 0 & 0 & 0 \\ 0 & 1 & 0 & 0 \\ 0 & 0 & 1 & 0 \\ 0 & 0 & 0 & 1 \end{bmatrix} = -\begin{bmatrix} 1 & 0 & 0 & 0 \\ 0 & \text{-}1 & 0 & 0 \\ 0 & 0 & \text{-}1 & 0 \\ 0 & 0 & 0 & \text{-}1 \end{bmatrix} + 2\begin{bmatrix} 1 & 0 & 0 & 0 \\ 0 & 0 & 0 & 0 \\ 0 & 0 & 0 & 0 \\ 0 & 0 & 0 & 0 \end{bmatrix}. \tag{4}$$

Adopting $(+, -, -, -)$ as the metrical signature (as we will throughout the article), we realize that we must have:

$$\bar{g}_{\mu\nu} = -g_{\mu\nu} + 2u_\mu u_\nu, \qquad \text{where} \qquad u_\mu = g_{\mu\nu}\frac{dx^\mu}{d\tau}. \tag{5}$$

Notice that both sides of the equality are covariant tensors that equal each other in one system, thus the equality

holds in every system.[5]

For later convenience, we may also derive an expression for the inverse absolute metric, defined by $\bar{g}^{\mu\rho}\bar{g}_{\rho\nu} = \delta^\mu{}_\nu$. By a contravariant argument, analogous to the covariant argument above, we find that the inverse absolute metric is given by:

$$\bar{g}^{\mu\nu} = -g^{\mu\nu} + 2u^\mu u^\nu. \tag{6}$$

That this is indeed the inverse of the absolute metric can be verified directly. It is a little surprising however that we get the inverse of the new metric by raising the indices with the *original* metric.[6]

In the new metric, proper intervals will be completely different from those in the original metric. Intervals as measured along a generating congruence line will however be the same; these are unaffected by the sign-flip. Using a bar to denote the four-velocity relative to the absolute metric, it then follows that

$$u^\mu = \bar{u}^\mu, \qquad u_\mu = \bar{u}_\mu. \tag{7}$$

Using this in Eq. (5), we immediately find

$$g_{\mu\nu} = -\bar{g}_{\mu\nu} + 2\bar{u}_\mu \bar{u}_\nu. \tag{8}$$

Comparing with Eq. (5), we see that there is a perfect symmetry in going from the original to the absolute metric, and vice versa.

V Freely falling observers as generators

As a specific example of the absolute metric, we again consider the line element of a radial line through a Schwarzschild black hole. We set $c = G = 1$, and introduce dimensionless coordinates, and proper intervals

$$x = \frac{r}{2M} \qquad t = \frac{t_{\text{original}}}{2M} \qquad \tau = \frac{\tau_{\text{original}}}{2M}. \tag{9}$$

The line element then takes the form

$$d\tau^2 = \left(1 - \frac{1}{x}\right)dt^2 - \left(1 - \frac{1}{x}\right)^{-1} dx^2. \tag{10}$$

As generators (u^μ) we consider freely falling observers, initially at rest at infinity. Using the squared Lagrangian formalism (see e.g. Ref. 1) for the equations of motion, we readily find the lowered four-velocity of the generating freefallers

$$u_\mu = \left(1, \frac{\sqrt{x}}{x-1}\right). \tag{11}$$

The absolute metric is then according to Eq. (5)

$$\bar{g}_{\mu\nu} = \begin{bmatrix} 1 + \frac{1}{x} & \frac{2\sqrt{x}}{x-1} \\[2ex] \frac{2\sqrt{x}}{x-1} & \frac{x(x+1)}{(x-1)^2} \end{bmatrix}. \tag{12}$$

To make an embedding of this metric we are wise to first diagonalize it by a coordinate transformation $t' = t + \phi(x)$. Letting $\frac{d\phi}{dx} = \frac{\bar{g}_{tx}}{\bar{g}_{tt}}$ the line element in the new coordinates becomes

$$d\bar{\tau}^2 = \left(1 + \frac{1}{x}\right)dt'^2 + \left(1 + \frac{1}{x}\right)^{-1} dx^2. \tag{13}$$

This metric is easy to remember since by chance it is the Schwarzschild metric with the minus signs replaced by plus signs (except for the minus sign in the exponent). Notice that nothing special happens with the metrical components at the horizon $(x = 1)$. At the singularity $(x = 0)$ however, the absolute metric is singular.

To produce a meaningful picture of this geometry, we must include the worldlines of the freely falling observers used to generate the absolute geometry. Coordinate transforming of the trajectories to the new coordinates t', x can be done numerically. The result is depicted in Fig. 11.
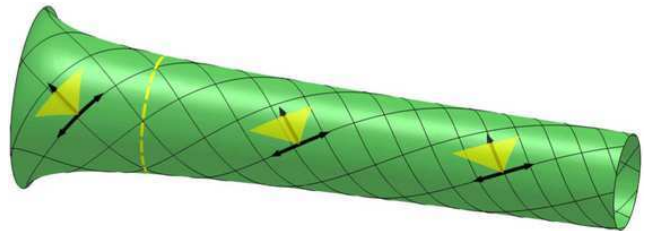

Figure 11: The absolute freefaller geometry. The dashed line is the horizon. As before the singularity lies outside of the embedding (towards the left).

Notice how the local Minkowski systems are twisted on the surface. The horizon lies exactly where the generating worldlines are at a 45° angle to a purely azimuthal line.

Time dilation is now not solely determined by the local embedding radius, but also by the gamma factor[7] of the observer at rest relative to the generating observer. For instance an observer at rest at the horizon will be at a 45° angle to the generating observer, corresponding to an infinite gamma factor, and his clock will therefore not tick at all during a Schwarzschild lap (one circumference), thus being infinitely time-dilated.

Unlike the hour-glass type embeddings of Sec. II B, this explanation of gravitational time dilation requires a basic knowledge of special relativistic time dilation. However, unlike the illustration of Fig. 7 where there is a cusp right at the horizon, Fig. 11 has the virtue of showing how passing the horizon is not at all dramatic (locally). Spacetime is as smooth and continuous at the horizon as everywhere else outside the singularity.

VI Symmetry-preserving generators

In this section we generalize the scheme outlined in the preceding section to include arbitrary two-dimensional (2D) metrics with a Killing symmetry,[8] for arbitrary generators that preserve manifest Killing symmetry. In two dimensions, the generating field u^μ can (since it is normalized) be specified by a single parameter as a function of x^μ. A parameter that is well suited to preserve the symmetries of the original metric is the *Killing* velocity v. By this we mean the velocity that a generator u^μ experiences for a Killing line (a worldline of constant x). In other words it is the velocity of a point of constant x as seen by the generating observer. The absolute value of this velocity will be smaller than one outside the horizon, and greater than one inside the horizon. Without loss of generality we can assume that the original line element is of the form $\mathrm{Diag}(g_{tt}(x), g_{xx}(x))$. The relation between u^μ and v is derived in Appendix A. The result is

$$u^\mu = \pm \sqrt{\frac{g_{tt}}{1-v^2}} \left(\frac{1}{g_{tt}}, \frac{-v}{\sqrt{-g_{xx}g_{tt}}} \right). \tag{14}$$

Using the lowered version of Eq. (14) in Eq. (5) gives us the absolute metric as a function of the parameter v. Making a coordinate transformation that diagonalizes this metric, analogous to the diagonalization in the preceding section,[9] yields after simplification

$$\bar{g}'_{\mu\nu} = \begin{bmatrix} g_{tt}\dfrac{1+v^2}{1-v^2} & 0 \\ 0 & -g_{xx}\dfrac{1-v^2}{1+v^2} \end{bmatrix}. \tag{15}$$

Notice that if there is a horizon present, where $g_{tt} = 0$, we have also $(1-v^2) = 0$. The quotient of these two entities will remain finite and well defined, given that $dv/dx \neq 0$ and $dg_{tt}/dx \neq 0$.

We see from Eq. (15) that there is much freedom in choosing $\bar{g}'_{tt}$. Since we can choose v arbitrarily close to 1, both inside and outside of the horizon, we can everywhere make $\bar{g}'_{tt}$ take an arbitrarily high value. Because the square root of $\bar{g}'_{tt}$ is proportional to the embedding radius, there are virtually no limits to what shape the curved surface can be given. To interpret the embedded surface we need also the generating worldlines, relative to the new (diagonalizing) coordinates. How these can be found is derived in Appendix B.

While the shape of the embedded surface depends strongly on the choice of generators, the *area* is independent of this choice. This holds regardless of any assumed symmetries as is explained in Appendix C.

VII Flat embeddings

Using Eq. (15) and assuming a time-symmetric and two-dimensional original metric, we can produce an absolutely flat absolute metric. This we can embed as a cylinder or a plane. We simply set $\bar{g}'_{tt} = C$, where C is some arbitrary positive constant. Solving for v yields

$$v = \pm\sqrt{\frac{C - g_{tt}}{C + g_{tt}}}. \tag{16}$$

As a specific example we consider a Schwarzschild original line element. We choose $v = 0$ at infinity, corresponding to the generating observers at infinity being at rest, which yields $C = 1$. We also choose the positive sign, corresponding to an in-falling observer (on the outside) to find

$$v = \frac{1}{\sqrt{2x - 1}}. \tag{17}$$

This is a completely smooth function at the horizon. We see that it remains real for $x \geq 1/2$. For other choices of C we can make the inner boundary come arbitrarily close to the singularity. We notice also that $\bar{g}'_{xx} = 1/C$ and is thus also constant. This means that the constant x-worldlines will be evenly spaced on the flat surface. Also we may, from the expression for v, immediately figure out how the local generator should be tilted relative to the constant x-worldline on the flat surface. An embedding for this particular case is displayed in Fig. 12.
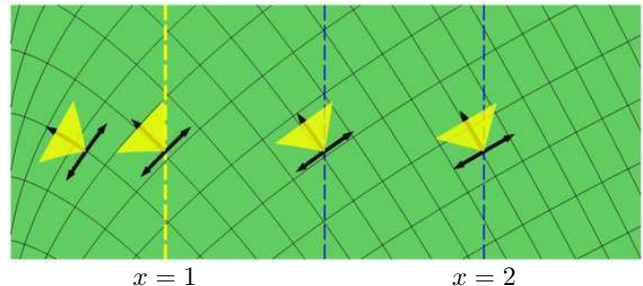

Figure 12: A flat embedding of a Schwarzschild black hole. The radial parameter x lies in the interval $[0.5, 2.5]$. We could equivalently embed this geometry as a cylinder. As we go further to the right (larger x), the lightcones will approach pointing straight up.

Notice that for this visualization the curvature of spacetime is manifested solely as a *twist* of the local Minkowski systems relative to each other. As in the case of Fig. 11, the flat embedding illustrates the smoothness of the spacetime around the horizon.

VIII Absolute geodesics

We know that the motion of particles in free fall corresponds to trajectories that maximize the proper time. Such trajectories can be found using the absolute scheme, as outlined above. The fact that these trajectories are also *straight*, is unfortunately a bit lost in this scheme. There

are however ways to manifestly retain at least parts of the original geodesic structure, in the absolute metric. The net value of this discussion turns out to be of more academic than pedagogical value. Below we therefore simply summarize the results derived in the appendices.

- Assuming an original 2D metric with a Killing symmetry, we can demand that *some* given motion $x(t)$ should be geodesic relative to the absolute metric. For example one can show that there exist generators such that outward-moving photons on a Schwarzschild radial line follow absolute geodesics. For brevity the analysis of this is omitted.

- To investigate the general connection between the geodesic structure of the original and the absolute metric, we derive a covariant expression for the absolute four-acceleration in terms of Lorentzian quantities. See Appendix D.

- Using the formalism of the preceding point we can show that if the generators are geodesics with respect to the original metric they will also be with respect to the absolute metric, and vice versa. See Appendix E. We also give an intuitive explanation for this.

- In the preceding points we have seen how some parts of the geodesic structure can be retained. To completely retain the geodesic structure, as is derived in Appendix F, we must have

$$\nabla_\alpha u_\mu = 0. \qquad (18)$$

At any *single* point in spacetime, this is easily achieved. We just go to an originally freely falling system and in this system choose $u^\mu = \frac{1}{\sqrt{g_{00}}}\delta^\mu{}_0$. Since in this system the metric derivatives all vanish, so will the derivatives of the generators.

For a normalized vector field u^μ to exist such that Eq. (18) holds everywhere, we must have a so called ultrastatic spacetime – as is derived in Appendix G. By ultrastatic we mean that space may have some fixed shape, but there can be no time dilation.

We conclude that only to a limited extent can we, in the absolute scheme, visualize Lorentz-geodesics as straight lines. There are however other visualization methods that are better suited for this, as discussed in Sec. XV.

IX   Charged black hole

All that we have done so far for ordinary black holes, in the absolute scheme, can also be done for charged black holes. The line element of a radial line is then given by (see e.g. Ref. 10)

$$d\tau^2 = \left(1 - \frac{1}{x} + \frac{\beta^2}{4x^2}\right)dt^2 - \left(1 - \frac{1}{x} + \frac{\beta^2}{4x^2}\right)^{-1}dx^2 \quad . (19)$$

The dimensionless constant β lies in the range $[0,1]$ and is proportional to the charge of the black hole. Just as in Sec. VII, we may find a flat absolute geometry for this line element as depicted in Fig. 13.
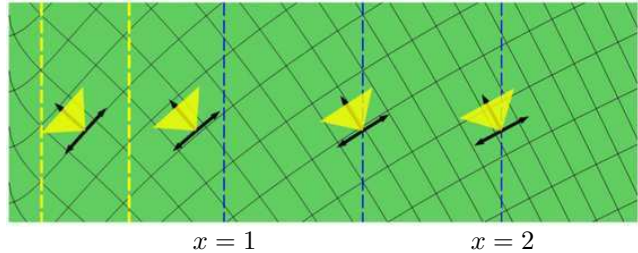

$x = 1$ \qquad\qquad $x = 2$

Figure 13: A flat embedding of a Reissner-Nordström black hole. The dimensionless radial coordinate x lies in the range $[0.22, 2.5]$. The two internal horizons are marked with the thicker dotted lines. The charge is chosen so that $\beta = 0.95$.

We see the classic three regions of the Reissner-Nordström solution. Thinking of free particles taking a path that maximizes the proper time we understand that a freely falling observer initially at rest in the innermost region, will accelerate towards the inner horizon. Actually this becomes clearer still if we form the absolute metric by simply taking the absolute value of the original metrical components, as we did in Sec. III. This corresponds to having generators that are orthogonal to the Killing field in the intermediate region, and parallel to the Killing field outside this region. See Fig. 14.
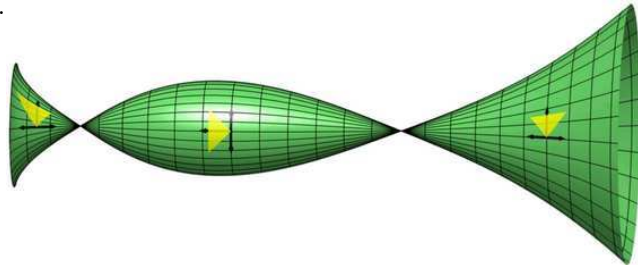

Figure 14: An alternative representation of a Reissner Nordström black hole. Notice the direction of the local Minkowski systems. Here $\beta = 0.995$ and the range is $[0.425, 0.7]$.

We notice that the spacetime geometry of the region just inside the inner horizon looks very much like the geometry just outside the outer horizon. Knowing that it takes a finite proper time to reach the outer horizon from the outside, we understand that it must take a finite proper time (while infinite coordinate time) to reach the innermost horizon from the inside. In the embedding there is however apparently no region to which the trajectory may go after it has reached the inner horizon. To resolve this puzzle, we must consider the extended Reissner-

Nordström solution. This is in principle straightforward, as will be briefly discussed at the end of Sec. XI.

X Flat spacetime

The simplest possible spacetime to which we may apply the absolute scheme, is flat Minkowski in two dimensions. Choosing a field of generating four-velocities that is constant, with respect to standard coordinates (t, x), the resulting absolute geometry is flat and can be embedded as a plane. If we choose some more disordered field of four-velocities we can however get an embedding with no apparent symmetries at all. There is however another choice of generators that will produce a regular surface,[11] as is illustrated in Fig. 15.
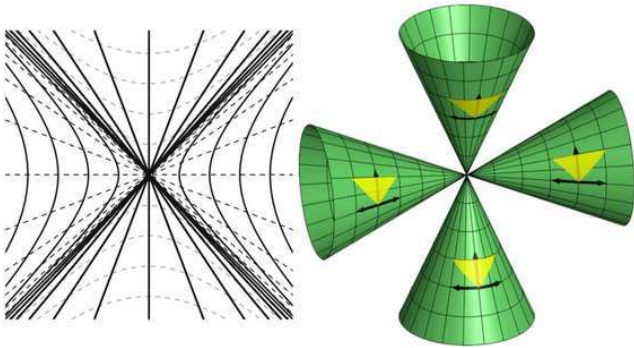

Figure 15: To the left: Minkowski spacetime with a certain set (as discussed in the main text) of worldlines (the thick full drawn lines). To the right: The corresponding absolute geometry embedding. Note that the conical surfaces are not closed as one goes around in the space direction, but rather they consist of very tightly rolled layers with no end.

In the right and left regions, of the Minkowski diagram, we have chosen so called Rindler observers as generators.[12] In the top and bottom regions we are using timelike geodesics converging at the origin as generators. The universe as perceived from this set of observers is known as a Milne universe (in two dimensions).[13]

It is obvious from the embedding that there is a (Lorentzian) Killing field directed around the conical surfaces. Imagining the corresponding field in the diagram, we realize that it is in fact the Killing field connected to continuous Lorentz transformations.

XI Extended black hole

Notice the similarity between the Kruskal diagram of a maximally extended Schwarzschild black hole (see e.g. Ref. 1) and the Rindler diagram to the left in Fig. 15. Having seen the interior and exterior regions of a (non–extended) black hole in the absolute scheme (Fig. 7), we

realize that we can also illustrate a maximally extended black hole (Fig. 16).
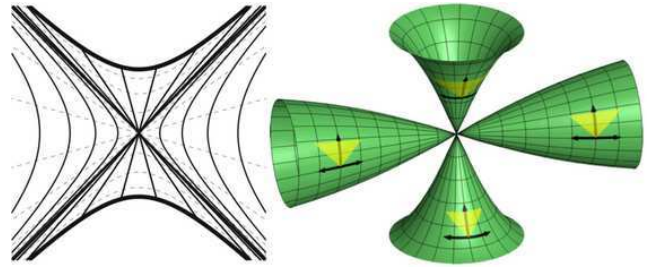

Figure 16: To the left: A Kruskal diagram of a maximally extended black hole. To the right: an embedding of the absolute geometry with generators at fixed radius in the exterior regions and at fixed Schwarzschild time in the interior regions (the full drawn lines in the diagram).

While all symmetries are preserved in this picture, it is hard to see how one can move between the different regions. Since the generators are null at the horizons, making the absolute distance along these lines zero, all the points along the null lines coming from the Kruskal origin sit at the connecting point in the embedding. Thus a trajectory passing one of the horizons in the diagram will pass through the connecting point in the embedding. However, where it will end up is not evident from the embedding alone. Through a more well behaved set of generators one can remove this obscurity at the cost of loosing manifest symmetry, as will be briefly discussed in Sec. XII.

Having seen the absolute version of the extended black hole, we can also figure out how the extended Reissner-Nordström black hole must look. At all the cusps in the embedding, four locally cone-like surfaces must meet. Otherwise, as is apparent from Sec. X, the spacetime will not be complete. I will leave to the readers imagination the specifics of how to extend the Reissner-Nordström embedding depicted in Fig. 14.

XII Other spacetimes

So far in the embedding examples, we have restricted ourselves to Lorentzian spacetimes with a Killing symmetry and also to generators that manifestly preserve this symmetry. The absolute scheme is however completely general. When applying the scheme to the Kruskal black hole, we do not have to let the generators be either parallel or orthogonal to the local Killing field, as we did before. Instead we could for instance use geodesic freefallers, originally at rest along a $t = 0$ line in the standard Kruskal coordinates. My best guess is that the corresponding embedding would resemble a tortoise shell.

We can also consider spacetimes where there is no Killing symmetry. As an example one could study a radial line through a collapsing thin shell of matter. (Here

there are local Killing fields but no global Killing field.) As a first try, one might choose observers at fixed x as generators. Outside of the shell we would (via the Birkhoff theorem) have a picture similar to Fig. 7. Inside the shell we would have a flat (though it may be rolled up) surface, with straight generating lines. Whether these two pieces can be put together in some meaningful manner I have yet to discover. Maybe one will find that another set of observers will be needed to join the two spacetime regions together.

XIII   Toy models

While we can use the absolute scheme to produce pictures representing exact solutions to Einstein field equations, we can also do the opposite. Suppose that we have a surface, say a plane, and we specify an angle as a function of position on the plane. Letting the angle correspond to the direction of the generators, it is straightforward to find the corresponding Lorentzian metric (just do the inverse transformation of Eq. (6)). We may insert this metric into some program (say Mathematica) and let it calculate the corresponding Einstein tensor and thus, through the field equations, also the energy-momentum tensor.[14] We may see the solution as a purely two-dimensional solution. Alternatively we may see it as a four-dimensional solution assuming that we add two dimensions corresponding to internally flat planes. In Fig. 17 we see an example of such a toy model spacetime.
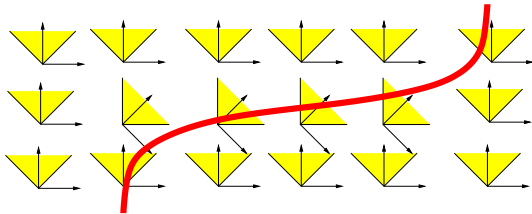

Figure 17: A crude illustration of a toy model for warp drive

From the look of the spacetime in Fig. 17 we might call the propulsion mechanism 'twist drive' rather than warp drive. I will leave to the readers imagination to visualize a spacetime that more deserves the name warp drive.

XIV   Other methods

In this article we have seen how one may use curved surfaces, with local Minkowski systems, to visualize for instance gravitational time dilation. This can also be achieved using a flat diagram, letting the space and time scales be encoded in the size (and shape) of the local lightcones as depicted in Fig. 18.

The disadvantage with this technique is that it is more abstract than the hourglass embedding (Fig. 4). In the
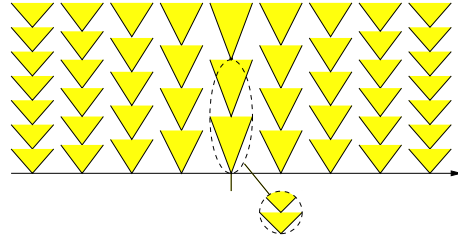

Figure 18: A flat spacetime visualization of a radial line through a star. The lightcones are everywhere, by definition, one proper time unit high, and two proper length units wide. The dashed circle illustrates that when we actually go to a specific region, the lightcones will appear as they do at infinity.

hourglass embedding there is a shorter distance between two Schwarzschild time lines inside the star than outside. From the flat lightcone model we must deduce this fact. Also one looses the visual connection to the concept of curved spacetime.

The flat diagram technique however has the virtue of being extendable to 2+1 dimensions. The scheme outlined in this article can also be used in 2+1 dimensions, but to produce a faithful image we would need a flat *absolute* spacetime. Then we could embed little lightcones of constant opening angle and size. To demand a Euclidean absolute spacetime is however quite restrictive, and it seems better to allow the lightcones to vary in apparent width and height. I will leave to the reader's imagination how this technique could be applied to visualize warp drive, rotating black holes, the Big Bang and so on.

XV   Comparison to other work

There are, to the author's knowledge, three other distinctly different techniques of visualizing curved spacetime using embedded surfaces.

Marolf[15] presents a way of embedding a two-dimensional Lorentzian metric in a 2+1 dimensional Minkowski spacetime (visualized as a Euclidean 3-space).

L. C. Epstein[16] presents a popular scientific visualization of general relativity. The underlying theory rests on the assumption of an original time independent, diagonal, Lorentzian line element. Rearranging terms in this line element one can get something that looks like a new line element, but where the proper time is now a coordinate. The 'space-propertime' can be embedded as a curved surface, from which many spacetime properties can be deduced.

In a previous article[17], I assumed a time independent Lorentzian line element. I then found another line element, also time symmetric, that is positive definite and geodesically equivalent to the original line element. The resulting geometry can be embedded as a curved surface as in Fig. 19. The method can be used to explain

straight lines in a curved spacetime, the meaning of forces as something that bends spacetime trajectories, etc.
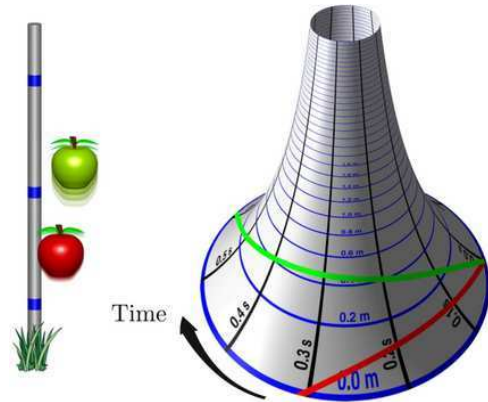

Figure 19: Illustration of how straight lines in a curved spacetime can explain the motion of upwards-thrown apples. The lines can be found using a little toy car that is rolled straight ahead on the surface.

Each of the three techniques outlined here together with the absolute scheme of this article has different virtues (and drawbacks). Depending on the audience they can all be used to explain aspects of the theory of general relativity.

XVI   Comments and conclusions

The absolute scheme as presented in this article, can be applied to *any* spacetime, giving a global positive definite metric. Together with the generating field of four-velocities, it carries complete information about the original Lorentzian spacetime.

While there are mathematical applications of this scheme (see Ref. 18), we have here focused on its pedagogical virtues. At the level of students of relativity, a study of the mathematical structure itself may have some pedagogical virtue. In particular it is instructive to see an alternative representation of the shape of spacetime.

The main pedagogical virtue is however that, applied to two-dimensional spacetimes, the absolute scheme enables us to make *embeddings* that illustrate the meaning of a curved spacetime.

While such an embedding is not unique, due to the freedom in choosing generators as well as the freedom of the embedding, it gives a completely faithful image of the true spacetime geometry. With only a basic understanding of Minkowski systems, a complete knowledge of the embedded parts of the Lorentzian geometry can be deduced from the surface. For instance we can figure out how much a clock has ticked along a certain path, or what path a thrown apple will take.

Also, many applications require no knowledge at all of special relativity. We do not need to mention Minkowski

systems or proper times to give a feeling for how geometry can explain how time can run at different rates at different places, or how space itself can expand. Most importantly we emphasize the point of view that gravity, according to general relativity, is about *shapes* – not forces and fields.

XVII   Questions for students of general relativity

Here are a handful of questions regarding applications of the absolute scheme. The answers are given in the next section.

1. The hour-glass shaped embedding of Fig. 4 illustrates a spacetime where time "runs slower" in a local region. How would a corresponding embedding look that illustrates how time can run faster in a local region?

2. Can you, using the technique of this article, illustrate a two-dimensional spacetime that is closed in space and time and with no vertices (by a vertex we mean a point from which the Minkowski systems point either outward or inward)?

3. Can a spacetime of the type specified in the preceding question be flat?

4. In exam periods students often need more time to study. Consider as a primary spacetime a flat plane with uniformly directed Minkowski systems. How would you alter this spacetime to ensure that there is sufficient time to study? Include the worldline of the student in need, as well as the worldline of the teacher bringing the exam.

5. Imagine an upright-standing cylindrical surface, with upward-directed Minkowski systems. The all-famous experiment where one twin goes on a trip and later returns to his brother, can be illustrated by two worldlines on the cylinder, one going straight up and the second going in a spiral around the cylinder (intersecting the first one twice). This scenario differs from the standard one in that no acceleration was needed by either twin for them to still reunite. The same question applies however. Will the twins have aged differently?

XVIII   Answers to students questions

Here are (the) answers to the questions of the preceding section.

1. Instead of a dip in the hour-glass shaped embedding (decrease of the radius towards the middle), we have a bulge (increase of radius towards the middle).

2. Yes. For instance a torus, with the Minkowski systems directed along the smaller toroidal circumference.

3. Yes. Make a tube out of a paper by taping two opposite ends together. Flatten the tube, preferably so that the tape is a bit away from the two folds that emerges. Roll the flattened tube, so that the tape describes a complete circle and connect the meeting paper ends by some more tape. If the local Minkowski systems on this shape are given a uniform direction, the corresponding Lorentz-geometry will be flat.

4. Make a sufficiently high and steep bump in the plane, while keeping the direction of the Minkowski systems (as seen from above the former plane). Make sure that the student's trajectory passes straight over the peak, while the teacher's trajectory misses it.

5. Oh yes. What time the twins experience is determined by their respective spacetime trajectories. If the trajectory of the traveling twin is tilted almost as much as a photon trajectory, he will have aged very little compared to his brother. There is also an article[19] that deals with this thought-experiment.

A   Finding u^μ as a function of v

Here is a derivation of the general expression for u^μ as a function of the Killing velocity v. Let us define v^μ as a vector perpendicular to u^μ, normalized to -1. Also we denote the Killing field by ξ^μ. The vectors as seen relative to a system comoving with u^μ are displayed in Fig. 20.
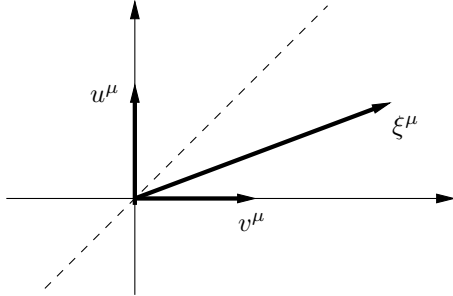

Figure 20: The Killing field in local coordinates comoving with u^μ.

We have then

$$\xi^\mu = (u^\mu + vv^\mu)K. \qquad (20)$$

Here the variable K may take positive or a negative values. Contracting both sides with themselves, we solve for K to find

$$K = \pm\sqrt{\frac{\xi^\alpha \xi_\alpha}{1 - v^2}}. \qquad (21)$$

The orthogonal vector v^μ can be expressed via

$$v^\mu = \frac{1}{\sqrt{g}}\epsilon^{\mu\rho}g_{\rho\alpha}u^\alpha \qquad \text{where} \qquad \epsilon^{\mu\rho} = \begin{pmatrix} 0 & -1 \\ 1 & 0 \end{pmatrix}. \quad (22)$$

Here $g = -\text{Det}(g_{\mu\nu})$. Through this definition v^μ is within $180°$ clockwise from u^μ (looking at the coordinate plane from above, assuming t up and x to the right). Inserting Eq. (22) into Eq. (20), using Eq. (21), we readily find

$$\left(\delta^\mu_{\ \nu} + \frac{v}{\sqrt{g}}\epsilon^{\mu\rho}g_{\rho\nu}\right)u^\nu = \pm\sqrt{\frac{1 - v^2}{\xi^\alpha \xi_\alpha}}. \qquad (23)$$

This is a linear equation for u^μ that can easily be solved. For the particular case of $g_{\mu\nu} = \text{Diag}(g_{tt}, g_{xx})$ and $\xi^\mu = (1, 0)$ we find

$$u^\mu = \pm\sqrt{\frac{g_{tt}}{1 - v^2}}\left(\frac{1}{g_{tt}}, \frac{-v}{\sqrt{-g_{xx}g_{tt}}}\right). \qquad (24)$$

So now we have a general expression for the generating four-velocity, expressed in terms of the Killing velocity v. The $\pm$ originates from the $\pm$ in the previous expression for K.

B   Vector transformation by diagonalization

Under the diagonalization of the absolute metric (as performed in Sec. VI) a general vector transforms according to

$$q'^\mu = \left(q^t + \frac{\bar{g}_{tx}}{\bar{g}_{tt}}q^x, q^x\right). \qquad (25)$$

Using the lowered version of Eq. (14) and the definition of the absolute metric, Eq. (5), we find after simplification

$$\frac{\bar{g}_{tx}}{\bar{g}_{tt}} = \frac{2v}{1 + v^2}\frac{-g_{xx}}{\sqrt{-g_{tt}g_{xx}}}. \qquad (26)$$

For the particular case of $q^\mu = u^\mu$, using Eq. (14), we find after simplification

$$u'^\mu = \pm\sqrt{\frac{g_{tt}}{1 - v^2}}\left(\frac{1}{g_{tt}}\frac{1 - v^2}{1 + v^2}, \frac{-v}{\sqrt{-g_{xx}g_{tt}}}\right). \qquad (27)$$

This expression can be used to find the generating lines in the new coordinates. We simply integrate u'^t and u'^x numerically, with respect to the parameter τ, to find $t'(\tau)$ and $x(\tau)$. These lines can then easily be mapped to an embedding of the absolute geometry.

C   Regarding the absolute area

Consider a small square in the coordinates we are using. Then consider two different choices of generators,

$u_1{}^\mu$ and $u_2{}^\mu$. Assume also that the coordinate square is small enough that the generating fields (as well as the metric) can be considered constant within the surface. We denote the absolute area of the coordinate square for the two representations by dA_1 and dA_2. Knowing that the absolute area is independent of the choice of coordinates we may evaluate each area in the local Minkowski systems $x_1{}^\mu$ and $x_2{}^\mu$, comoving with the corresponding generator. In these systems the original square will be deformed, but the absolute area will exactly equal the coordinate area. Since the two Minkowski systems are related via the Lorentz transformation, which preserves coordinate areas, we know that the coordinate areas are equal and thus also $dA_1 = dA_2$. Because the argument applies to arbitrary pairs of generators, it follows that the absolute area is independent of the choice of generators.

In N dimensions we can, by a completely analogous argument, show that the N-volume of the absolute metric is independent of the choice of generators.

D Covariant relation for the absolute four-acceleration

First we derive an expression for a general absolute four-velocity $\bar{q}^\mu$, in terms of Lorentzian quantities

$$
\begin{aligned}
\bar{q}^\mu &= \frac{dx^\mu}{d\bar{\tau}} = \frac{dx^\mu}{d\tau}\frac{d\tau}{d\bar{\tau}} \\
&= q^\mu \sqrt{\frac{g_{\mu\nu}dx^\mu dx^\nu}{-g_{\mu\nu}dx^\mu dx^\nu + 2u_\mu u_\nu dx^\mu dx^\nu}} \\
&= q^\mu \sqrt{\frac{1}{-1 + 2u_\mu u_\nu \dfrac{dx^\mu}{d\tau}\dfrac{dx^\nu}{d\tau}}} \\
&= q^\mu \frac{1}{\sqrt{2(u_\mu q^\mu)^2 - 1}} \ .
\end{aligned} \tag{28}
$$

Notice that choosing $q^\mu = u^\mu$ yields $\bar{u}^\mu = u^\mu$ as we realized before.

To covariantly relate the absolute four-acceleration to the Lorentzian quantities we need an expression for the absolute affine connection, i.e. the affine connection for the absolute metric

$$
\bar{\Gamma}^\mu_{\alpha\beta} = \frac{1}{2}\bar{g}^{\mu\rho}\left(\partial_\alpha \bar{g}_{\rho\beta} + \partial_\beta \bar{g}_{\rho\alpha} - \partial_\rho \bar{g}_{\alpha\beta}\right). \tag{29}
$$

Using the corresponding definition of the original affine connection, together with the expressions for the absolute metric and its inverse given by Eqs. (5) and (6), we can write this as

$$
\begin{aligned}
\bar{\Gamma}^\mu_{\alpha\beta} = \Gamma^\mu_{\alpha\beta} &- 2u^\mu u^\rho \Gamma_{\rho\alpha\beta} + (\text{-}g^{\mu\rho} + 2u^\mu u^\rho) \\
&\times \left(\partial_\alpha(u_\rho u_\beta) + \partial_\beta(u_\rho u_\alpha) - \partial_\rho(u_\alpha u_\beta)\right).
\end{aligned} \tag{30}
$$

Now we evaluate $\frac{\bar{D}\bar{q}^\mu}{\bar{D}\bar{\tau}}$ in an *originally* freely falling system where the original affine connection vanishes. Setting all

unbarred derivatives to their covariant analog and using the definition of covariant derivatives, Eqs. (28) and (30) we obtain

$$
\begin{aligned}
\frac{\bar{D}\bar{q}^\mu}{\bar{D}\bar{\tau}} =\ & \frac{1}{\sqrt{2(u_\mu q^\mu)^2 - 1}}\frac{D}{D\tau}\left(\frac{q^\mu}{\sqrt{2(u_\mu q^\mu)^2 - 1}}\right) \\
&+ 2\frac{q^\alpha q^\beta}{2(u_\mu q^\mu)^2 - 1}\left(-g^{\mu\rho} + 2u^\mu u^\rho\right) \\
&\times (u_\beta \bigtriangledown_\alpha u_\rho + u_\rho \bigtriangledown_\alpha u_\beta - u_\beta \bigtriangledown_\rho u_\alpha).
\end{aligned} \tag{31}
$$

Here we have a manifestly covariant relation. We can expand this expression, and simplify it somewhat using

$$
u^\mu u_\mu = 1 \qquad u^\mu \bigtriangledown_\alpha u_\mu = 0 \qquad k \equiv u^\mu q_\mu. \tag{32}
$$

The first two relations follow directly from the normalization of u^μ, and the latter is a definition introduced for compactness. The resulting expansion is given by

$$
\begin{aligned}
\frac{\bar{D}\bar{q}^\mu}{\bar{D}\bar{\tau}} =\ & \frac{2}{2k^2 - 1} \\
& \Big[\frac{1}{2}\frac{Dq^\mu}{D\tau} - \frac{kq^\mu}{2k^2 - 1}(q^\rho q^\sigma \bigtriangledown_\sigma u_\rho + u_\rho\frac{D}{D\tau}q^\rho) \\
& - kq^\alpha \bigtriangledown_\alpha u^\mu + u^\mu q^\beta q^\alpha \bigtriangledown_\alpha u_\beta \\
& + kq^\alpha \bigtriangledown^\mu u_\alpha - 2ku^\mu q^\alpha u^\rho \bigtriangledown_\rho u_\alpha \Big].
\end{aligned} \tag{33}
$$

E Geodesic generators

Consider a trajectory that everywhere is tangent to the generating field so that $q^\mu = u^\mu$. Also, assume that the generators are geodesics $\frac{Du^\mu}{D\tau} = 0$, or equivalently $u^\rho \bigtriangledown_\rho u^\mu = 0$. Using the normalization relation $u^\mu u_\mu = 1$, from which it follows that $u^\mu \bigtriangledown_\alpha u_\mu = 0$, we immediately see that Eq. (31) reduces to

$$
\frac{\bar{D}\bar{u}^\mu}{\bar{D}\bar{\tau}} = 0. \tag{34}
$$

Thus if the original generators are geodesic then they are geodesic also relative to the absolute metric. Through the perfect symmetry in transforming from the absolute to the Lorentzian metric and back, we have derived implicitly that if the absolute generators are geodesics they will also be geodesics in Lorentzian spacetime. We conclude that *if and only if* the original generators are geodesic then they will be geodesic in the absolute spacetime.

To get an intuitive feeling for the result we just derived consider a straight generating line (in the absolute sense) on an embedded surface. Any small deviation from this line will introduce negative contributions to the proper time. A rigorous argument is that an infinitesimal variation of a trajectory (with fixed endpoints), around a straight generating line, will to first order in the variation parameter not affect the *absolute* length of the trajectory. Also we know that the Lorentzian distance along a trajectory is shorter than or equal to the absolute distance (the equality holds if and only if we follow a generator).

Hence we cannot gain proper time to first order in the variational parameter as we vary the trajectory. Thus the Lorentz proper time is maximized by the original trajectory.

On the other hand, if the absolute generating line is curving relative to the surface, it seems plausible that we could gain proper time by taking a path on the *outside* of the curving generating line. Thus a non-geodesic absolute generator would imply a non-geodesic Lorentzian generator. The result that the generators are absolute geodesics if and only if they are Lorentzian geodesics, is thus intuitively understandable.

F Deriving necessary and sufficient conditions for geodesic equivalence

To investigate if it is possible to completely retain the original geodesic structure in the absolute metric, we set $\frac{\bar{D}\bar{q}^\mu}{\bar{D}\bar{\tau}} = 0$ and $\frac{Dq^\mu}{D\tau} = 0$ in Eq. (33). The resulting equation is given by

$$0 = -\frac{kq^\mu}{2k^2 - 1} q^\rho q^\sigma \bigtriangledown_\sigma u_\rho - kq^\alpha \bigtriangledown_\alpha u^\mu + u^\mu q^\beta q^\alpha \bigtriangledown_\alpha u_\beta$$
$$+ kq^\alpha \bigtriangledown^\mu u_\alpha - 2ku^\mu q^\alpha u^\rho \bigtriangledown_\rho u_\alpha. \quad (35)$$

If this equation is to hold for *all* directions, q^α, it must hold for the particular case $q^\alpha = u^\alpha$. Inserting this and using the normalization of u^μ, only the second term survives

$$u^\alpha \bigtriangledown_\alpha u^\mu = 0. \quad (36)$$

Thus it is *necessary* to have geodesic generators to get all the geodesics 'right'. Assuming the generators to be geodesic – the last term in Eq. (35) dies. Multiplying the remaining four terms by q_μ, we are after simplification left with another necessary constraint

$$\left(\frac{-k}{2k^2 - 1} + k \right) q^\alpha q^\mu \bigtriangledown_\alpha u_\mu = 0. \quad (37)$$

The expression within the parenthesis is zero if and only if $k = \pm 1$. Assuming a future-like convention on both u^μ and q^μ we cannot have a negative k, and $k = 1$ corresponds uniquely to $u^\mu = q^\mu$, a direction that we already considered. Thus, the expression outside the parenthesis must vanish. For this to hold for *all* directions q^α, we must have

$$\bigtriangledown_\alpha u_\mu = - \bigtriangledown_\mu u_\alpha. \quad (38)$$

Using this necessary antisymmetry in Eq. (35) we are left with

$$0 = -kq^\alpha \bigtriangledown_\alpha u^\mu + kq^\alpha \bigtriangledown^\mu u_\alpha. \quad (39)$$

Lowering this with $g_{\mu\nu}$ and using the necessary antisymmetry again, we obtain

$$q^\alpha \bigtriangledown_\alpha u_\nu = 0. \quad (40)$$

For this in turn to hold for *all* q^α it is necessary to have $\bigtriangledown_\alpha u_\mu = 0$. This also immediately satisfies the above necessary constraints on antisymmetry and generator geodesics. That it is also *sufficient* for geodesic equivalence follows directly from Eq. (35). Thus the absolute metric will be geodesically equivalent to the original one, if and only if

$$\bigtriangledown_\alpha u_\mu = 0. \quad (41)$$

G Proving that $\bigtriangledown_\mu u_\nu = 0$ everywhere implies ultrastatic spacetime

Assuming $\nabla_\mu u_\nu = 0$, the Frobenius condition[20] $u_{[\mu}\nabla_\nu u_{\rho]} = 0$ is trivially satisfied. This means that there exists (locally) a slice for which u^μ is normal. Introducing coordinates such that $t = $ const in every slice and letting the spatial coordinates follow the congruence connected to u^μ, the line element takes the form

$$g_{\mu\nu} \begin{bmatrix} g_{tt} & 0 \\ & \\ 0 & g_{ij} \end{bmatrix}. \quad (42)$$

In this particular system $u_\mu = \sqrt{g_{tt}}\, \delta^t{}_\mu$. Then we readily find

$$\bigtriangledown_\alpha u_\beta \equiv \partial_\alpha u_\beta - \Gamma^\rho_{\alpha\beta} u_\rho \quad (43)$$
$$= ... \quad (44)$$
$$= \frac{1}{\sqrt{g_{tt}}}$$
$$\left(\delta^t{}_\beta (\partial_\alpha g_{tt}) - \frac{1}{2} \left(\partial_\alpha g_{t\beta} + \partial_\beta g_{t\alpha} - \partial_t g_{\alpha\beta} \right) \right). \quad (45)$$

Letting i and j denote general spatial indices and evaluating this equation for $\alpha = t, i$ and $\beta = t, j$ (there are four different combinations) we readily find

$$\partial_\mu g_{tt} = 0 \quad (46)$$
$$\partial_t g_{ij} = 0. \quad (47)$$

Thus in these particular coordinates, choosing a t-labeling such that $g_{tt} = 1$, the metric takes the form

$$g_{\mu\nu} = \begin{bmatrix} 1 & 0 \\ & \\ 0 & g_{ij}(\mathbf{x}) \end{bmatrix}. \quad (48)$$

A spacetime where the metric can be put in this form is called ultrastatic. Thus $\bigtriangledown_\mu u_\nu = 0$ implies an ultrastatic spacetime. The converse, choosing the preferred observers in the ultrastatic spacetime as observers, is also obviously true.

References

[1] R. D'Inverno, *Introducing Einstein's Relativity*, (Oxford Univeristy Press, Oxford 1998), pp. 99-101.

[2] Eq. (1) defines a so called distance function, or a metric. It can also be used considering events where $dx > cdt$. Then $d\tau^2$ is negative which simply means that it is related to spatial distance rather than temporal distance. A distance function like Eq. (1) corresponds to a flat spacetime, but see Eq. (10) for an example of a distance function corresponding to a curved spacetime.

[3] S. Weinberg, *Gravitation and cosmology* (John Wiley & sons, New York, 1972), pp. 337-338.

[4] Assuming that there is no black hole inside the crust.

[5] As was pointed out to me by Ingemar Bengtsson, this relation is also used by Hawking & Ellis (Ref. 18), although for completely different purposes than those of this article.

[6] If we had instead considered a metric of the form $-g^{\mu\nu} + \alpha u^\mu u^\nu$, where α is some general number, the inverse would have been $-g^{\mu\nu} + \alpha/(\alpha - 1)u^\mu u^\nu$. It is only in the case $\alpha = 2$ that we can simply raise the indices of the absolute metric with the original metric to get the inverse of the absolute metric.

[7] The gamma factor is defined as $\gamma = (1-v^2)^{-\frac{1}{2}}$ where v is the relative velocity. With this definition, it follows from Eq. (1) that $d\tau = \frac{dt}{\gamma}$.

[8] A geometry has a Killing symmetry if there exists a vector field (called a Killing field) ξ^μ such that when we shift our coordinates $x^\mu \rightarrow x^\mu + \epsilon\xi^\mu$ – the metric has the same form. As an example we can consider a geometry that can be embedded as a curved surface. Then there exists a Killing field directed around the surface (in the azimuthal direction) with a length proportional to the embedding radius. Also, if there are coordinates where the metric is independent of one coordinate, then there is a Killing symmetry with respect to that coordinate.

[9] $t' = t + \phi(x)$ where $\frac{d\phi}{dx} = \frac{\bar{g}_{tx}}{\bar{g}_{tt}}$ gives $\bar{g}'_{\mu\nu} =$ Diag$(\bar{g}_{tt}, \bar{g}_{xx} - \frac{(\bar{g}_{tx})^2}{\bar{g}_{tt}})$

[10] C. W. Misner, K. S. Thorne, J. A. Wheeler, *Gravitation* (W. H. Freeman and Company, New York, 1973), p. 841.

[11] Suggested to me by Sebastiano Sonego.

[12] W. Rindler, *Relativity: Special, General and Cosmological* (Oxford University Press, Oxford, 2001), pp. 267-272.

[13] W. Rindler, *Essential Relativity: Special, General and Cosmological* (Springer Verlag, New York, 1977), pp. 204-207.

[14] This may well violate the energy conditions.

[15] D. Marolf, "Spacetime Embedding Diagrams for Black Holes," Gen. Relativ. Gravit., **31**, 919-944 (1999).

[16] L. C. Epstein, *Relativity Visualized* (Insight Press, San Francisco, 1994), chaps. 10-12.

[17] R. Jonsson, "Embedding Spacetime via a Geodesically Equivalent Metric of Euclidean Signature," Gen. Relativ. Gravit. **33**, 1207-1235 (2000).

[18] S. W. Hawking and G. F. R. Ellis, *The large scale structure of space-time*, (Cambridge University Press, Cambridge, 1973), p. 39.

[19] T. Dray, "The twin paradox revisited," Am. J. Phys. **58**, 822-825 (1989).

[20] The Frobenius condition in explicit form reads: $u_\mu(\nabla_\nu u_\rho - \nabla_\rho u_\nu) + u_\rho(\nabla_\mu u_\nu - \nabla_\nu u_\mu) + u_\nu(\nabla_\rho u_\mu - \nabla_\mu u_\rho) = 0$.